Available online at www.sciencedirect.com
SCIENCE DIRECT®
Journal of Power Sources 140 (2005) 250–257
JOURNAL OF POWER SOURCES
www.elsevier.com/locate/jpowsour

Performance of polymer electrolyte membrane fuel cells with carbon nanotubes as oxygen reduction catalyst support material

N. Rajalakshmi[b], Hojin Ryu[b], M.M. Shaijumon[a], S. Ramaprabhu[a,*]

[a] *Alternate Energy Technology Laboratory, Department of Physics, Indian Institute of Technology Madras, Chennai 600036, India*
[b] *Advanced Material Division, Korea Research Institute of Chemical Technology, Daejeon, Korea*

Received 1 July 2004; accepted 23 August 2004
Available online 27 October 2004

Abstract

Platinum/carbon nanotubes (Pt/CNT) electrocatalysts are prepared. The CNTs are pre-treated in order to obtain reactive sites for the adherence of Pt metal particles. The electrocatalysts are characterized by scanning electron micrograph (SEM), transmission electron micrograph (TEM) and X-ray photoelectron spectrum (XPS) measurements. It is found that the catalysts contain both Pt(0) and Pt(IV) species. A high Pt loading of 32.5% on CNTs is obtained when the catalysts are prepared with ethylene glycol and Pt salt. The electrocatalysts are used for the oxygen reduction reaction in polymer electrolyte membrane fuel cells (PEMFCs) and the performance of PEMFC is analyzed with respect to catalyst synthesis and Pt loading. Cyclic voltammetric studies show that the Pt utilization in the fuel-cell electrodes is around 44%. Catalysts obtained with mild nitric acid-treated CNTs give a better performance of 680 mV at 500 mA cm^{-2} and 600 mV at 800 mA cm^{-2} than catalysts prepared with ethylene glycol and Pt salt.

Keywords: Carbon nanotubes; Support material; Electrocatalyst; Proton exchange membrane fuel cell; Cyclic voltammetry; Ethylene glycol

1. Introduction

Carbon nanotubes (CNTs) are a subject of great interest given their unique structure and excellent properties. They offer potential applications in electronic devices, catalysts, sensors, field-emission devices and hydrogen-storage media [1–8]. The size and morphology of CNTs enable them to be a suitable catalyst support, in which active metal particles may disperse on the external walls or be encapsulated in the interior of the nanotubes. The metal particles on the external walls make contact with the reactant molecules more easily than those encapsulated inside the internal channels of the CNTs [9–12].

There are different methods for dispersing platinum on carbon. Since CNTs are chemically inert, activating their surfaces is essential and this has motivated numerous studies to improve metal dispersions on carbons, mainly through optimization of the metal supporting procedures or functionalization of the carbon surface. The aromatic ring system of the carbon nanotubes can be disrupted by the application of extremely aggressive reagents, such as HNO_3 or H_2SO_4 or a mixture of two, and therefore the nanotubes can be functionalized with groups such as hydroxyl (–OH), carboxyl (–COOH) and carbonyl (>C=O) that are necessary to anchor metal ions to the tube. Sonication in organic solvents produces dangling bonds that undergo further chemical reactions and provide the oxidative power necessary to incorporate acidic sites into carbon nanotubes, which varies with the tube diameter [13–16].

The electrocatalytic mass activity of Pt clusters in a periodic array of ordered nanoporous carbon is higher than that of platinum in carbon black samples, and thus the former are suitable for oxygen reduction [17]. Lordi et al. [18] reported the preparation of metal-loaded single-walled CNTs (SWNTs) by a three-step process, namely (i) strong oxidation

* Corresponding author. Tel.: +91 44 22578680; fax: +91 44 22570509.
E-mail address: ramp@iitm.ac.in (S. Ramaprabhu).

0378-7753/$ – see front matter © 2004 Elsevier B.V. All rights reserved.
doi:10.1016/j.jpowsour.2004.08.042

in nitric acid to purify the tubes; (ii) weak oxidation to anchor sites (surface oxides) for Pt; (iii) attachment of Pt to the SWNTs by reduction of K_2PtCl_4 in ethylene glycol. The surface oxides have mostly carboxylic acid functions and act as anchors for Pt particles, presumably through an ion-exchange reaction in a reducing agent, to produce material that consists of 10 wt.% Pt with particles sizes averaging between 1 and 2 nm. Other strategies including electrostatic deposition and physisorption of nanoparticles of Au, Pt and Ag on to acid-treated multi-walled CNTs (MWNTs), where the nanoclusters rapidly tend to coalesce on the nanotube templates and result in wire-like structures that consist of large polycrystals. Choi et al. [19] reported the spontaneous reduction of metal ions on the sidewalls of carbon nanotubes in an ethanolic aqueous solution of Na_2PtCl_4, where the nanotube/Pt^{2+} systems can be categorized as redox pairs. This process differs from electroless deposition that requires reducing agents or a catalyst, as a result of direct redox reactions between ions and nanotubes. Although these studies strongly support the application of carbon nanomaterials as catalyst supports in the electrodes of fuel-cells, actual fuel-cell tests have yet to be undertaken.

The performance of a direct methanol fuel cell (DMFC) with Pt-loaded MWNTs obtained by the reduction of Pt ion salt in ethylene glycol solution has shown that the concentration of ethylene glycol plays a key role in the deposition of Pt particles [20]. Liu et al. [21] studied the preparation and characterization of Pt-based electrocatalysts on MWNTs for a proton exchange membrane fuel cell (PEMFC) by a two-step sensitisation–activation treatment. It was found that the deposition of Pt was very sensitive to the ageing of the sensitization solution. Steigerwalt et al. [22] studied six Pt/Ru–carbon nanofibre composites for methanol oxidation in DMFC.

As part of an ongoing investigation of synthetic strategies for preparing Pt-loaded CNTs as oxygen reduction catalysts, the study reported here is a systematic preparation and characterization of Pt catalysts supported on MWNTs with PEMFC test results. Each catalyst-supported MWNT is prepared by a different method, and the catalyst synthesis procedures have been optimized to produce an appreciable loading of catalyst in the support to provide measurable performance as PEMFC oxygen reduction catalysts. The PEMFC electrodes are prepared in a uniform fashion with the intention of evaluating the catalyst synthesis procedure that might show the best performance in actual fuel-cell operation. The effects of different synthesis procedures of Pt on MWNTs and the loading of Pt on PEMFC performance are analyzed by maintaining the same experimental conditions.

2. Experimental section

2.1. Synthesis of carbon nanotubes

MWNTs were synthesized by catalytic decomposition of acetylene using Mischmetal-based AB_2 alloy hydrides as the catalyst [23]. The as-synthesized carbon nanotubes were refluxed with concentrated HNO_3 for 24 h, followed by washing with de-ionized water several times and then the sample was dried in air for 30 min at 100 °C. They were further treated with hydrofluoric (HF) acid. This was followed by air oxidation at 500 °C for 2 h to remove the amorphous carbon and to open the ends of the carbon nanotubes. The samples were characterized by SEM and TEM measurements.

2.2. Electrocatalyst synthesis

Catalyst A: Catalytic Pt nanoparticles with MWNTs were prepared by immersion of MWNTs into a solution of 75 mM H_2PtCl_6. After magnetic stirring for about 12 h, the platinum salt was reduced by slowly adding a solution that was a mixture of 0.1M $NaBH_4$ and 1M NaOH. When the reaction was complete, the solution was filtered with copious amounts of deionized water, filtered and dried by vacuum filtration using cellulose membrane filters with a pore size of 0.1 μm. The recovered carbon nanotubes loaded with platinum were then dried at 80 °C for about 2 h.

Catalyst B: In order to increase the 'wetness' of the CNTs surfaces for the adherence of metal particles, catalyst samples were prepared by sonication of 150 mg of purified CNTs in 20 ml of acetone for 6 h. A solution containing MWNTs was magnetically stirred for 24 h, after adding an aqueous solution of hexachloroplatinic acid (1%). The reducing solution was added slowly to the mixture containing MWNTs and Pt salt. Then, the solution was washed with copious amounts of deionized water and acetone for many times, and filtered. The solid portion was dried at 80 °C for about 3 h.

Catalyst C: This was prepared by the same method as for catalyst A, except that the MWNTs were functionalized by pre-treatment with 70% nitric acid in order to introduce surface oxides. A sample of 200 mg of MWNTs was refluxed under constant agitation in 30 ml of 70% HNO_3 at 110 °C for 12 h. The solid phase was removed by centrifugation and washed with distilled water; the recovered MWNTs were dried at 80 °C for 12 h. The dried sample was ultrasonicated in 10 ml of acetone for 1 h and then 1% hexachloroplatinic acid solution was added slowly during stitrring. After 12 h, the mixture was reduced by adding a reducing solution of 0.1M $NaBH_4$ and 1M NaOH.

Catalyst D: This was prepared by weak oxidation of purified carbon nanotubes in nitric acid to create anchor sites, i.e., surface oxides for the Pt. Then, Pt was attached to the surface of the oxidized nanotubes by reduction of K_2PtCl_6 in ethylene glycol, which probably achieved ion exchange with the hydrogen atoms on the carboxylic acid sites on the surfaces of the CNTs. In a typical synthesis, 100 mg of CNTs with 22 mg of K_2PtCl_6 was refluxed with 300 ml diluted ethylene glycol (3:2 molar ratio with water) for 6 h at 110 °C. Following reflux, the mixture was allowed to cool to room temperature and then centrifuged for 30 min at 5000 rpm. The wet solids were washed many times with deionized water, filtered and dried at 80 °C for 4 h.

2.3. Electrochemical measurements

For characterization of the electrocatalysts towards oxygen reduction in a solid PEMFC, membrane electrode assemblies (MEA) were obtained by sandwiching a pre-treated Nafion 1035 membrane between the anode and cathode. Both the anode and cathode layer consisted of a backing layer, a diffusion layer and a catalyst layer. To prepare the catalyst layer, the required amount of catalyst was mixed with a 5% Teflon suspension. The mixture was suspended in water and ultrasonicated by adding 5 wt.% Nafion solution. The paste thus obtained was brushed on to Teflonized carbon paper GDL-10 (10-H, SGL carbon group technologies, Sigracet) and pressed at 130 °C and 1000 psi for 2 min. The anode contained a Pt loading of 0.25 mg cm^{-2} and the cathode 0.5 mg cm^{-2}. The operating conditions were kept constant to facilitate a comparative evaluation of the various MEAs. The anode and cathode were contacted on their rear with gas flow-field plates that were machined from high-density graphite blocks (Electrochem, USA), in which channels were machined to achieve minimum mass polarization in the PEMFC. Humidified gases are passed to the electrodes from a Novatech test station. Adjacent to both the graphite blocks, gold-coated current-collectors are used and are connected to a Won A-Tech (HPCS 1) dc load box via a suitable software for various cycles of current loading and for activating the electrode. Galvanostatic polarization data were obtained at various temperatures. The geometric area of the electrode was 5 cm^2.

Cyclic voltammetry (CV) was used to measure the electrochemical surface area (ESA) of the fuel-cell electrodes, in order to obtain the localization of platinum near their front surfaces, using an EG&G M270 electrochemical system. On passing argon for the test electrode and hydrogen through the counter electrode chamber, the potential was swept between 0 and 1.2 V versus a reversible hydrogen electrode (RHE) at a scan rate of 15 mV s^{-1}. Because of the negligible overpotential for hydrogen oxidation or evolution at the counter electrode, it serves as a hydrogen reference electrode. From the CV, the charge equivalent to the area under the hydrogen desorption region was evaluated and the ESA was calculated assuming that the charge required for the adsorption–desorption of a monolayer of atomic hydrogen on the surface is 210 μC cm^{-2} [24].

3. Results and discussion

3.1. Characterization of MWNTs and Pt catalysts

Scanning electron micrographs of purified MWNTs and Pt-loaded MWNTs (catalyst A) are shown in Fig. 1a and b, respectively. It can be seen that the tubular walls are sufficiently decorated by Pt nanoparticles with a particle size-distribution in the range 3–15 nm. Similar micrographs pictures were taken for the other catalysts B, C and D. The energy dispersive analysis in Fig. 2a–d shows that the amount of Pt loaded on the carbon nanotube support with reference to carbon can be evaluated qualitatively as 14.5, 16.2, 19.6 and 32.5% for catalysts A, B, C and D, respectively (Table 1).

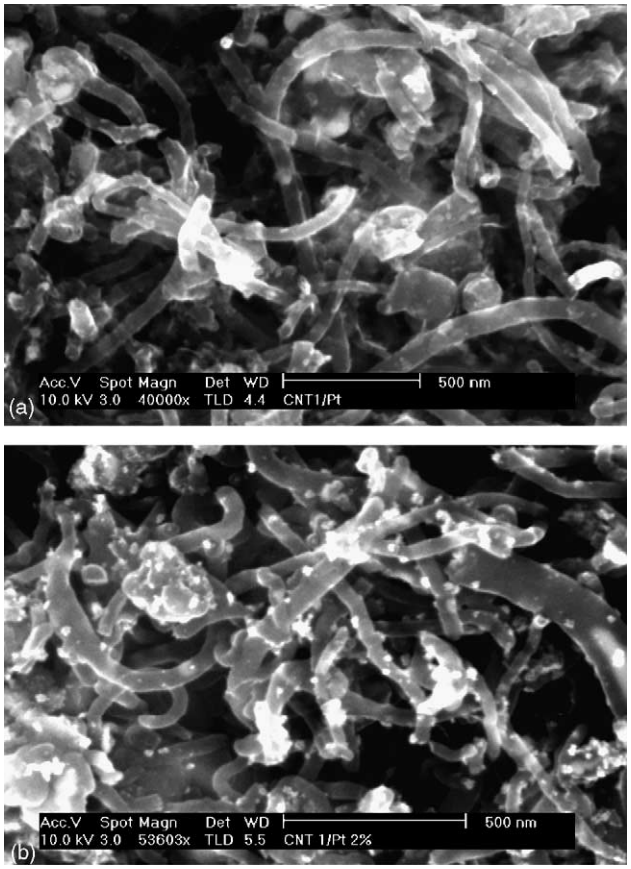

Fig. 1. (a) Scanning electron micrographs of (a) purified MWNTs and (b) platinum dispersed on MWNTs support.

TEM measurements were performed by ultrasonicating the sample in acetone for 1 h to obtain a good dispersion and then deposition on to copper grids covered with a continuous film of carbon. A HRTEM image of purified MWNTs is presented in Fig. 3. A TEM image of Pt-loaded CNT for catalyst C is given in Fig. 4 and shows a more or less uniform distribution of noble metal particles of size of about 3–5 nm on the CNTs. TEM images of other catalysts also reveal uniform distribution of Pt nanoparticles, except for catalyst D where agglomeration occurs with a maximum particle size of 12–15 nm. The particle size of Pt may be correlated with the oxidation of CNTs, which indicates that the efficient deposition of Pt nanoparticles is due to a strong interaction between the metal salt precursor and the graphene edges of the CNTs. Chemical functional groups, namely –COOH and –OH derived from chemical oxidation processes, act as anchoring sites for metal nanoparticles. These –COOH sites induce the impregnation of small and large particles (broad distribution). From the TEM measurements, it is observed that, for oxidized CNTs, the diameter of the metal particles deposited is less than that of non-oxidized CNTs.

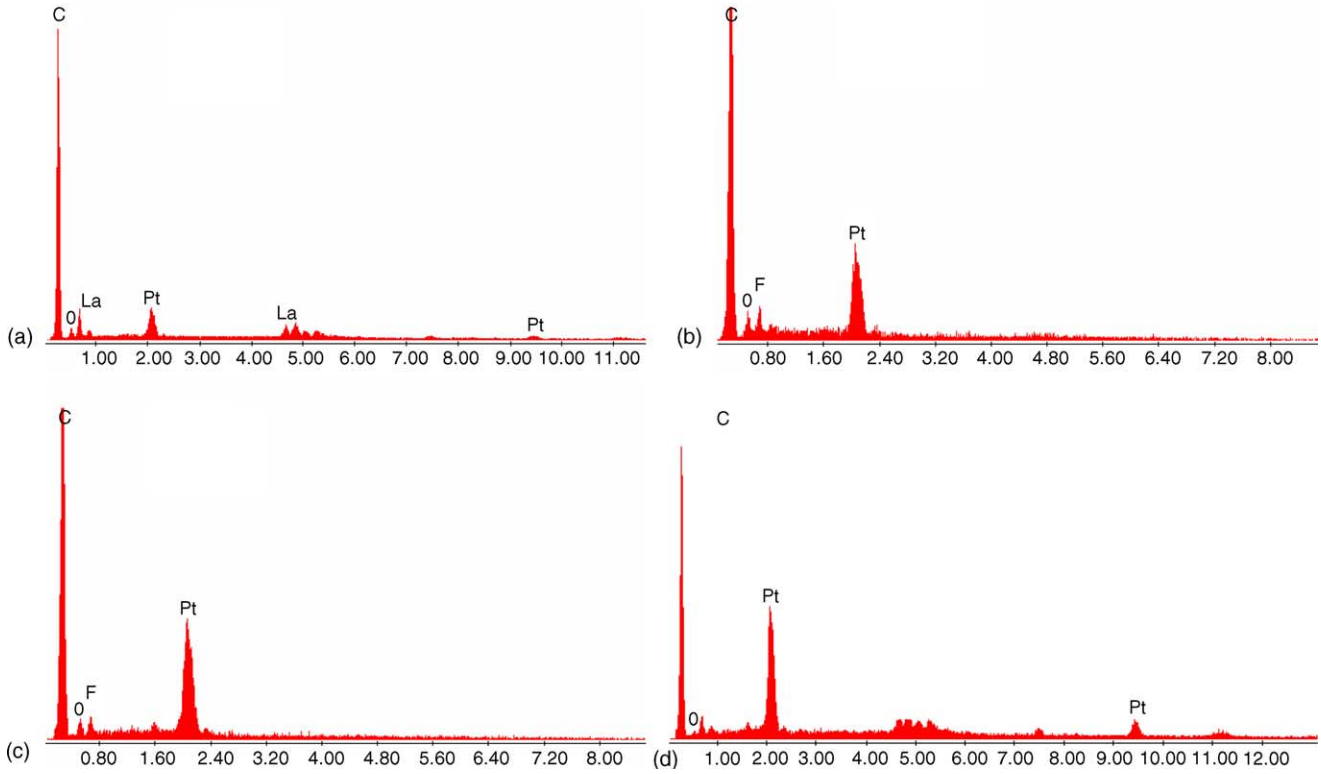

Fig. 2. Energy dispersive analysis of (a) catalyst A prepared with aqueous medium, (b) catalyst B prepared with organic solvent, (c) catalyst C pre-treated with nitric acid, and (d) catalyst D prepared by ethylene glycol method.

The XPS spectrum of purified MWNTs is given in Fig. 5a. The O 1s peak at 533.7 eV shows the oxidized CNTs in comparison with pure pristine surface, for which the peak occurs at 531 eV. This higher binding energy indicates that the electrons are more strongly bound to the surface carbon. The C 1s spectrum, deconvoluted into two peaks is presented in Fig. 5b. The peak at 288.9 eV shows that the surfaces are covered with carboxylic groups.

The Pt 4f core level XPS spectrum of Pt-loaded CNTs is shown in Fig. 6. The doublet contains a peaks at 71.4 and 74.7 eV, i.e., there is a spin-orbit splitting of 3.3 eV for the different Pt oxidation states of the Pt(0) and Pt(IV) species. The lower binding energy doublet with Pt $4f_{7/2}$ at 71.4 eV agrees well with the published value of 71.1 eV for Pt. The spectrum was deconvoluted using a curve-fitting program into four components labeled as 1, 2, 3 and 4 with respective binding energies of 71.3, 72.4, 74.3 and 75.7 eV and respective relative intensities of 81, 18, 62 and 37%. The signals at 71.3 eV can be assigned to zero-valent Pt, the signal at 72.4 eV is ascribed to PtO, and the signals at 74.3 and 75.7 eV seemingly arise from PtO_2 species [25–27].

3.2. Electrochemical measurements

The current–voltage characteristics of a PEMFC fabricated with nanocomposites of Pt on MWNTs as a cathode catalyst were obtained by activating the electrodes between the open-circuit potential and increasing the current as shown in Fig. 7. The same procedure was followed for all the catalysts, prior to polarization studies. This activation cycle is necessary to activate the catalyst for the oxygen reduction reaction [28]. The polarization curves for fuel-cell electrodes prepared using catalysts A, B, C and D, respectively, at various temperatures ranging from 50 to 80 °C under an operating

Table 1
Platinum loading, PEMFC performance and kinetic parameters of various catalysts

Sample	Pt (%)	CNT (%)	Pt loading (%)	Tafel slope (mV/decade)	Resistance (Ω cm^2)	Voltage (mV) at 500 mA cm^{-2}
Catalyst A	13.3	77.97	14.5	82.5	0.31	630
Catalyst B	14.5	75.15	16.2	61.5	0.35	640
Catalyst C	18.4	75.65	19.6	75.1	0.21	676
Catalyst D	28.6	59.51	32.5	56.7	0.41	638
E Tek	20	100	20	90.5	0.198	686

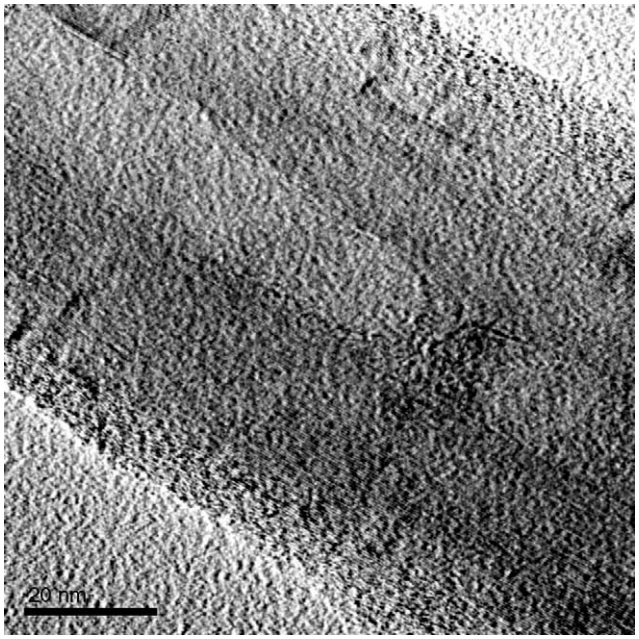

Fig. 3. Transmission electron micrograph of purified MWNTs.

pressure of 15 psi are given in Fig. 8a–d. Under the same operating conditions, the fuel-cell performance is almost the same for all the catalysts up to a current density of 400 mA cm^{-2}, giving a potential of 750 mV. But at a slightly higher current density of 500 mA cm^{-2}, however, the electrode prepared with catalyst C gives a potential of 680 mV, whereas the other electrodes with catalysts A, B and D give around 640 mV as shown in Fig. 9. A commercial 20% Pt on C catalyst also reports 680 mV. The oxygen reduction reactivity, which is reflected in the performance of the fuel-cell, can be attributed to the different particle size of Pt on the Pt/MWNTs catalysts, which results from the different preparation methods. TEM analysis shows a homogeneous distribution of smaller Pt particles distribution for catalyst C, which results in an enhanced interaction between the Pt and CNT and thus leads to higher performance. The data of Fig. 9 show that catalyst C, for which the CNTs were pre-treated with nitric acid to assist the adherence of metal particles, gives a better performance at higher current densities compared with all the other catalysts. Thus, although catalyst D has higher Pt loading than catalyst C, viz., 32 wt.% versus 19.6 wt.%, the fuel-cell performance at higher current densities is lower than that of catalyst C. This can be attributed to the larger

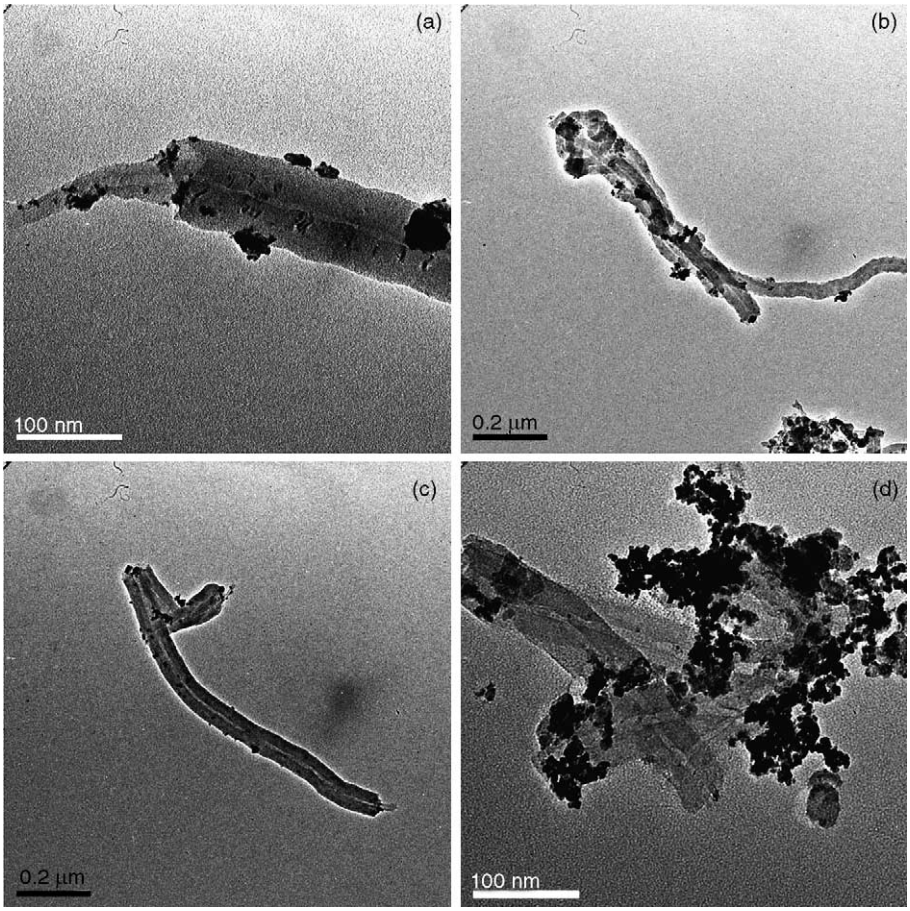

Fig. 4. Transmission electron micrographs of (a) catalyst A, (b) catalyst B, (c) catalyst C, and (d) catalyst D.

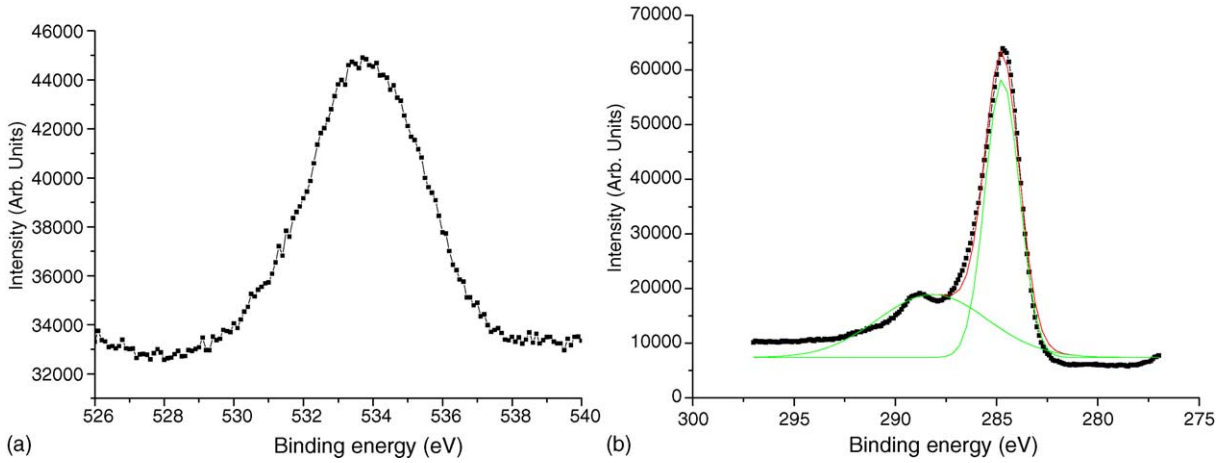

Fig. 5. X-ray photoelectron spectrum of purified MWNTs for (a) oxygen 1s state and (b) carbon 1s state.

particle size and higher agglomeration of the Pt particles in catalyst D.

The relative PEMFC performance depends strongly on the electrical conductivity of the CNT support, and the ability of the catalyst support to transport electrons to the current collector of the MEA. In the region of low current density, the voltage drops in the polarization curve, which are generally known as the activation polarization, reflects the sluggish kinetics of the oxygen reduction reaction at the cathode surface. The experimental polarization data were analyzed using the semi-empirical equation proposed by Ticianelli et al. [29], i.e.,

$$V = V_0 - b \log I - RI \quad (1)$$

where V and I are the experimentally measured cell voltage and current, respectively; b and R are the Tafel slope and total dc resistance. The dc resistance constitutes the contributions from the membrane resistance and other electrode components that are responsible for the linear variation of potential with current. The membrane resistance is found to be 0.1072 $\Omega\,cm^2$ for a membrane of thickness 89 μm. The experimental data were fitted to the above equation by a non-linear least squares method in order to evaluate the kinetic parameters of the different electrocatalysts from regression analysis. The resulting values are given in Table 1. It is clear that high performance is obtained with a high loading of Pt up to 19%, which naturally shows a low dc resistance. The Tafel slope ($dV/d(\log I)$) for oxygen reduction is found to be around 50–90 mV per decade over the entire current density range for the synthesized catalysts.

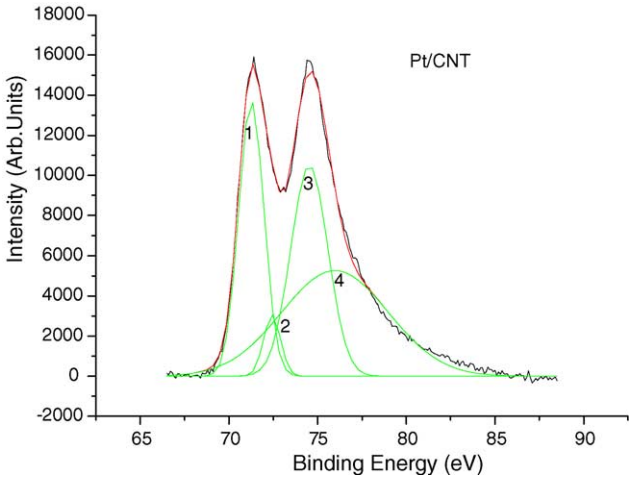

Fig. 6. X-ray photoelectron spectrum of Pt/CNTs for Pt 4f state.

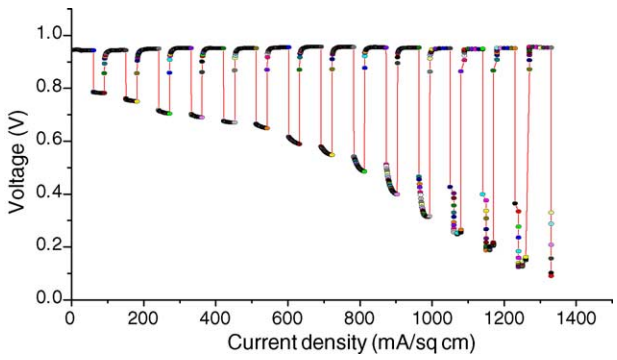

Fig. 7. Activation cycle for PEMFC electrode.

The electrocatalysis of O_2 reduction using the Pt nanoparticle electrodes was also examined. Nanostructured carbons with such high electrocatalytic activity are expected to be useful for the construction of fuel-cell cathodes in which high Pt loading is essential. The cyclic voltammetry data presented in Fig. 10 show that Pt is localized on the electrode surface, i.e., hydrogen adsorption and desorption that occurs on a Pt surface can be seen in the range 0–0.4 V. To evaluate the Pt surface area, the current densities of hydrogen adsorption and desorption were integrated separately and referred to a charge of 210 $\mu C\,cm^{-2}$ [24], which is assumed to relate to a monolayer of hydrogen adsorption on the Pt surface. The oxygen reduction current is found to be 7 mA for Pt-loaded CNTs

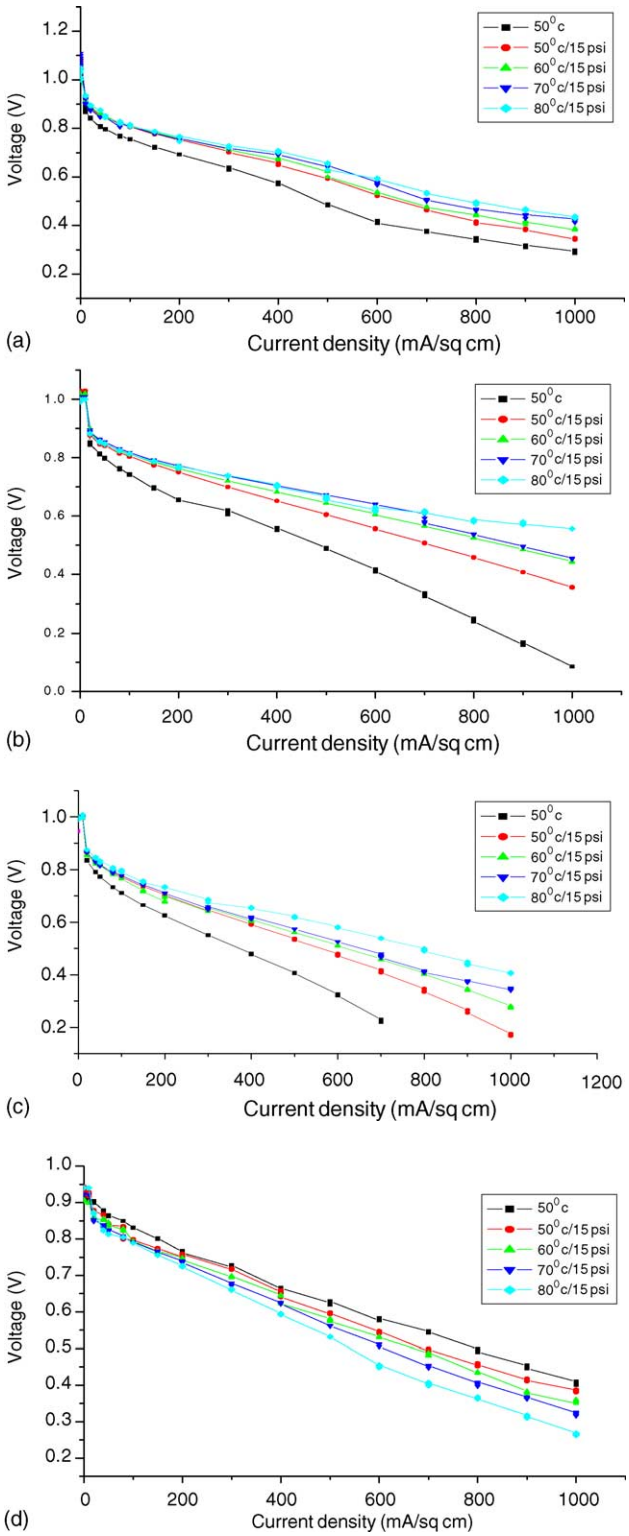

Fig. 8. Polarization curves of PEMFC performance at various temperatures and pressures for catalysts A, B, C and D.

at potentials characteristic for Pt electrocatalysis. There are two ways to express the catalytic activity, namely (i) mass activity, i.e., the current per unit amount of catalyst; (ii) the specific activity i.e., for unit surface area of catalyst. The mass

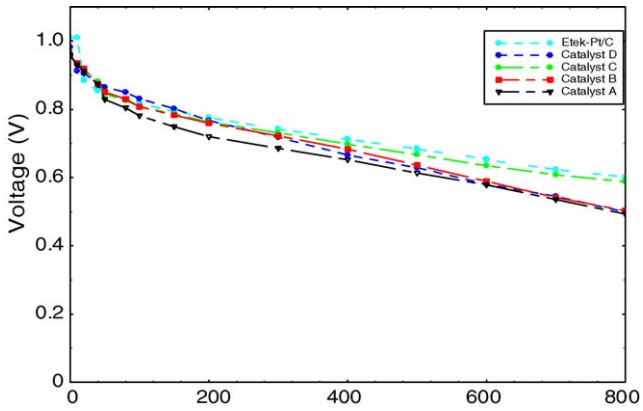

Fig. 9. Comparison of fuel-cell performance with various catalysts and with commercial catalyst at 80 °C and 15 psi.

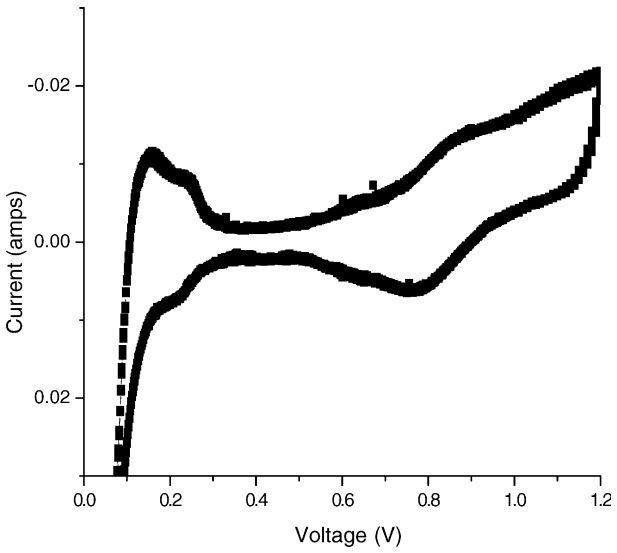

Fig. 10. Cyclic voltammogram illustrating electrocatalytic nature of Pt dispersed on CNTs (scan rate 15 mV s^{-1}, geometric area 5 cm^2).

activity has practical implications in fuel-cells, because the cost of the electrode depends on the amount of Pt used, and specific activity provides a measure of the electrocatalytic activity of Pt atoms in the particle surface. A Pt utilization of around 44% was found for all the catalysts.

4. Conclusion

Electrocatalysts have been prepared using Pt salts as a source of metal and pre-treated CNTs. They have been used for the oxygen reduction reaction in a PEMFC and the resulting performance has been analyzed with respect to catalyst synthesis and Pt loading. Electrodes prepared with the catalyst pre-treated with HNO_3 for the oxidation of CNTs give a Pt loading of 19.6% and a higher performance for fuel-cell applications. By contrast, eletrodes prepared with the catalyst obtained by ethylene glycol and Pt salt give a Pt loading

of 32% with lower fuel-cell performance, which is due to the larger Pt particle size and agglomeration. Thus, for high performance in fuel-cells, CNTs have to be functionalized to have a uniform dispersion with a narrow Pt particle range, rather than a higher loading of platinum.

Acknowledgements

The authors would like to thank KRICT, Daejeon for the support of this work. One of the authors (NR) is grateful to the Korea Federation of Science and Technology for a fellowship under the Brain Pool Program. MMS is thankful to IITM, Chennai and DRDO, Government of India.

References

[1] P.M. Ajayan, S. Iijima, Nature 361 (1993) 333.
[2] T. Hertel, R. Martel, P. Avouris, J. Phys. Chem. B 102 (1998) 910.
[3] S.S. Wong, J.D. Harper, P.L. Lansbery, C.M. Lieber, J. Am. Chem. Soc. 120 (1998) 603.
[4] A.C. Dillon, K.M. Jones, T.A. Bekkedahl, C.H. Kiang, D.S. Bethune, M.J. Heben, Nature 386 (1997) 377.
[5] N. Rajalakshmi, K.S. Dhathathreyan, B.C. Sathish Kumar, A. Govinda Raj, Electrochem. Acta 45 (2000) 4511.
[6] G. Gundiah, A. Govindaraj, N. Rajalakshmi, K.S. Dhathathreyan, C.N.R. Rao, J. Mater. Chem. 13 (2003) 209.
[7] H. Dai, J.H. Hafner, A.G. Rinzler, D.T. Colbert, R.E. Smalley, Nature 384 (1996) 147.
[8] S. Hynek, W. Fuller, J. Bentley, Int. J. Hydrogen Energy 22 (1997) 601.
[9] G. Che, B.B. Lakshmi, C.R. Martin, E.R. Fisher, Langmuir 15 (1999) 750.
[10] B. Rajesh, K.R. Thampi, J.M. Bonard, B. Viswanathan, J. Mater. Chem. 10 (2000) 1757.
[11] R.M. Lago, S.C. Tsang, K.L. Lu, Y.K. Chen, M.L.H. Green, J. Chem. Soc., Chem. Commun. (1955) 1355.
[12] L.M. Ang, T.S.A. Hor, G.Q. Xu, C.H. Tung, S.P. Zhao, J.L.S. Wang, Carbon 45 (2000) 134.
[13] E.T. Michelson, I.W. Chiang, J.L. Zimmermann, P.J. Boul, J. Lozano, J. Liu, R.E. Smalley, R.H. Hauge, J.L. Margrave, J. Phys. Chem. B 103 (1999) 4318.
[14] M. Holzinger, O. Vostrovsky, A. Hirsch, F. Hennrich, M. Kappes, R. Weiss, F. Jellen, Angew. Chem. Int. Ed. 40 (2001) 4002.
[15] V. Georgakilas, K. Kordatos, M. Prato, D.M. Guldi, M. Holzinger, A. Hirsch, J. Am. Chem. Soc. 124 (2002) 760.
[16] S. Niyogi, M.A. Hamon, H. Hu, B. Zhao, P. Bhowmik, R. Sen, M.E. Itkis, R.C. Haddon, Acc. Chem. Res. 35 (2002) 1105.
[17] S.H. Joo, S.J. Choi, I. Oh, J. Kwak, Z. Liu, O. Terasaki, R. Ryoo, Nature 412 (2001) 169.
[18] V. Lordi, N. Yao, J. Wei, Chem. Mater. 13 (2001) 733.
[19] H.C. Choi, M. Shim, S. Bangsaruntip, H. Dai, J. Am. Chem. Soc. 124 (2002) 9058.
[20] W. Li, C. Liang, W. Zhao, J. Qiu, Z. Zhou, G. Sun, Q. Xin, J. Phys. Chem. B 107 (2003) 6292.
[21] A. Liu, X. Lin, J.Y. Lee, W. Zhang, M. Han, L.M. Gan, Langmuir 18 (2002) 4054.
[22] E.S. Steigerwalt, G.A. Deluga, C.M. Lukehart, J. Phys. Chem. B 106 (2002) 760.
[23] M.M. Shaijumon, N. Rajalakshmi, H. Ryu, S. Ramaprabhu, Diamond Relat. Mater., in preparation.
[24] T. Biegler, D.A.J. Raud, R. Woods, J. Electroanal. Chem. Interfac. Electrochem. 29 (1971) 269–277.
[25] J. Knecht, G. Stark, Fransius, Anal. Chem. 289 (1978) 206.
[26] A.K. Shukla, K.V. Ramesh, R. Manoharan, P.R. Sarode, S. Vasudevan, Ber. Bunsen-Ges. Phys. Chem. 89 (1985) 1261.
[27] J.S. Hammond, N. Winograd, J. Electroanal. Chem. 78 (1977) 55.
[28] A.K. Shukla, M. Neergat, B. Parthasarathi, V. Jayaram, M.S. Hegde, J. Electroanal. Chem. 504 (2001) 111.
[29] E.A. Ticianelli, C.R. Derouin, A. Redondo, S. Srinivasan, J. Electrochem. Soc. 135 (1988) 2209.